Pleiotropy Modulates the Efficacy of Selection in *Drosophila melanogaster*

Christelle Fraïsse,*[,1] Gemma Puixeu Sala,[1] and Beatriz Vicoso*[,1]
[1]Institute of Science and Technology Austria, Am Campus 1, Klosterneuburg 3400, Austria
***Corresponding authors:** E-mails: christelle.fraisse@ist.ac.at; bvicoso@ist.ac.at
Associate editor: Joanna Kelley

Abstract

Pleiotropy is the well-established idea that a single mutation affects multiple phenotypes. If a mutation has opposite effects on fitness when expressed in different contexts, then genetic conflict arises. Pleiotropic conflict is expected to reduce the efficacy of selection by limiting the fixation of beneficial mutations through adaptation, and the removal of deleterious mutations through purifying selection. Although this has been widely discussed, in particular in the context of a putative "gender load," it has yet to be systematically quantified. In this work, we empirically estimate to which extent different pleiotropic regimes impede the efficacy of selection in *Drosophila melanogaster*. We use whole-genome polymorphism data from a single African population and divergence data from *D. simulans* to estimate the fraction of adaptive fixations (α), the rate of adaptation (ωA), and the direction of selection (*DoS*). After controlling for confounding covariates, we find that the different pleiotropic regimes have a relatively small, but significant, effect on selection efficacy. Specifically, our results suggest that pleiotropic sexual antagonism may restrict the efficacy of selection, but that this conflict can be resolved by limiting the expression of genes to the sex where they are beneficial. Intermediate levels of pleiotropy across tissues and life stages can also lead to maladaptation in *D. melanogaster*, due to inefficient purifying selection combined with low frequency of mutations that confer a selective advantage. Thus, our study highlights the need to consider the efficacy of selection in the context of antagonistic pleiotropy, and of genetic conflict in general.

Key words: **(mal)adaptation, pleiotropy, selective constraint, evo-devo, gene expression, *Drosophila melanogaster*.**

Article

Introduction

Natural selection should ensure that only mutations that are beneficial become fixed in a population, whereas deleterious ones are removed. However, the efficacy of selection can be reduced by several factors, leading to the fixation of deleterious mutations and loss of beneficial ones. The best understood is a reduction in the effective population size, *Ne*, which exacerbates the effect of genetic drift (Kimura and Ohta 1971, Chapter I; Maynard 1976). Differences in effective population size can occur between species, populations, and even genomic regions. For instance, population bottlenecks, as well as high levels of inbreeding, can lead to strong reductions of the effective size of a population (Nei et al. 1975). Similarly, Hill–Robertson effects (Hill and Robertson 1966), the interference of selective effects between partially linked sites, can reduce *Ne* in genomic regions of low recombination and/or high density of functional sites (Elyashiv et al. 2016; Campos et al. 2017; Booker and Keightley 2018).

Another facet of selection efficacy concerns the nature of new mutations themselves. For instance, selection on recessive mutations will be largely inefficient until these are at a frequency high enough that homozygous individuals are common, which may lead to a sieve against new recessive beneficial mutations (Haldane 1927; Marad et al. 2018). Such mutations should be more effectively selected on X chromosomes, which are haploid in males (Charlesworth et al. 1987; Vicoso and Charlesworth 2009). Second, although mutations are traditionally categorized as beneficial, neutral or deleterious, they can also have a context-dependent effect on fitness, if they bring an advantage only to a specific tissue, sex or life stage, but are otherwise deleterious. Because of these potentially antagonistic pressures, pleiotropic genes, which affect different phenotypes, likely evolve under unusual selective scenarios (Connallon and Hall 2018). Specifically, pleiotropic mutations have been predicted to be under stronger purifying selection, as selection will act on many phenotypes at once (Kimura and Ohta 1974; Van Dyken and Wade 2010). On the other hand, if a new mutation affects many phenotypes, adaptation may be strongly limited (Fisher 1930; Collet et al. 2018), and divergence at that locus may be primarily driven by drift.

The best-studied case of antagonistic pleiotropy, sexual antagonism, occurs when the functional divergence of males and females leads to sex-specific optima for phenotypes expressed in both sexes (Darwin 1871). As males and females share essentially the same genome, mutations favorable in one sex may be deleterious to the other. Thus, it may be difficult for the sexes to reach their own fitness optima, leading to a so-called gender load in sexual populations (e.g., in beetles: Arnqvist and Tuda 2010). Evidence for sexual antagonism in animals and plants is accumulating (Bonduriansky and Chenoweth 2009), and experiments in *Drosophila* have shown that sexually antagonistic variation occurs genome-

wide (Rice 1992; Innocenti and Morrow 2010). The resolution of sexual conflict is expected to involve mechanisms that decouple developmental pathways between the sexes, such as sex-biased expression (Ellegren and Parsch 2007; VanKuren and Long 2018). The pervasive expression divergence between the sexes found in many organisms has consequently been interpreted as potential evidence of past sexual conflict (Parsch and Ellegren 2013). Many studies in *Drosophila* (Zhang et al. 2004; Pröschel et al. 2006; Grath and Parsch 2012; Perry et al. 2014; Avila et al. 2015) and in other taxa (e.g., nematodes: Cutter and Ward 2005; mammals: Torgerson et al. 2002; Good and Nachman 2005; algae: Lipinska et al. 2015) have further found a faster rate of evolution of male-biased genes, possibly due to a relaxation of pleiotropic constraints (Meisel 2011; Parsch and Ellegren 2013).

Developmental pleiotropy has also been well characterized, especially in *Drosophila* (Davis et al. 2005; Artieri et al. 2009) and *Caenorhabditis elegans* (Cutter and Ward 2005). It implies that genes expressed early during development will be more evolutionary constrained than genes expressed later, because they may be involved in a higher number of functional interactions. This model echoes another pleiotropic model used to explain the evolution of aging, first expressed by Williams (1957) and experimentally validated by Rose and Charlesworth (1980), which assumes the existence of pleiotropic alleles that increase fitness more strongly early in life than they decrease it later (see Lemaître et al. 2015 for a review). Altogether, these models highlight the potential pervasiveness of antagonistic pleiotropy in nature and its importance in evolution.

Understanding how selective pressures shape genome evolution has been a main goal of evolutionary genomics, and many tests of the efficacy of selection in different species and genomic regions have been performed (see Booker et al. 2017 for a review). A commonly used measure is α (Smith and Eyre-Walker 2002), the proportion of divergent sites fixed by positive selection, which can be estimated from the number of synonymous and nonsynonymous sites that differ within and between species. If selection is efficient and adaptive evolution dominates, α should approximate one, whereas if selection is too inefficient for adaptive mutations to become fixed and deleterious mutations to be removed, α should be strongly reduced. In genes evolving primarily under strong purifying selection, α should also be close to zero. To understand whether differences in α are due to changes in purifying selection or in positive selection, the rate of adaptive substitutions relative to the rate of neutral evolution (ωA) can additionally be estimated (Bierne and Eyre-Walker 2004; Gossmann et al. 2010; Galtier 2016). Another estimate related to α is the direction of selection (*DoS*, Stoletzki and Eyre-Walker 2011), which is zero under neutrality, and negative and positive under purifying and positive selection, respectively. Finally, many studies simply use the ratio of nonsynonymous to synonymous divergence (*Dn*/*Ds*) or polymorphism (*Pn*/*Ps*) to assess selective pressures: *Dn*/*Ds* should increase under positive selection, and both *Dn*/*Ds* and *Pn*/*Ps* should decrease under purifying selection. These empirical studies have consistently detected a reduced efficacy of selection in regions of low recombination (Campos et al. 2014; Charlesworth and Campos 2014; Castellano et al. 2016) and in species with lower effective population size (Jensen and Bachtrog 2011; Bataillon et al. 2015; Galtier 2016; but see Bachtrog 2008 and Andolfatto et al. 2011 for counterexamples). Similarly, α values for X-linked genes are consistently larger than for autosomal genes (Meisel and Connallon 2013), even when differences in recombination are accounted for (Campos et al. 2018; Charlesworth et al. 2018).

Although increased purifying selection against pleiotropic mutations (McGuigan et al. 2014) and slow rates of evolution of pleiotropic genes (Salathé et al. 2006) have been observed, the overall effect of pleiotropy on selection efficacy is not as well understood. Some studies found reduced rates of adaptation and/or efficacy of selection for more pleiotropic genes (Hahn and Kern 2005; Papakostas et al. 2014), whereas others found the opposite (Vedanayagam and Garrigan 2015; Huber et al. 2017; Josephs et al. 2017), or no effect at all (Jordan et al. 2003; Hahn et al. 2004). One challenge in making sense of these studies is that pleiotropy can be interpreted in many ways (Paaby and Rockman 2013), and different measures are used to estimate it. Common measures include the number of protein–protein interactions, a proxy for the number of molecular functions of a gene, as well as the breadth of expression, which reflects the potential of a gene to affect different phenotypes. Both of these suffer from the drawback of not directly assessing whether the gene has an effect on more than one fitness component (e.g., a gene may perform the same function in many tissues, or have a single molecular function in a very large gene network).

Finally, a last challenge faced by all these studies is the fact that many parameters influencing the efficacy of selection are themselves correlated (e.g., expression and nonneutral divergence, recombination and expression, connectivity and expression, etc.; see supplementary fig. S1, Supplementary Material online), making it difficult to disentangle their individual effects. In particular, studies of pleiotropy rarely take into account recombination, and generally focus on one type of pleiotropic antagonism (e.g., between sexes, life stages, tissues, or gene networks). Similarly, although many studies have detected faster adaptive evolution of male-biased genes, it is difficult to disentangle the effect of reduced pleiotropy from increased rates of adaptation due to sexual selection, the favored hypothesis.

Here, we take a systematic approach to examine the effect of pleiotropy on the efficacy of selection in *Drosophila melanogaster*. First, we consider the effect of well-known modulators of selection efficacy, such as X-linkage, recombination rate and expression level, on different measures of positive and purifying selection (α, *DoS*, ωA, *Pn*/*Ps*, *Dn*/*Ds*). We then combine these with various proxies for pleiotropy: gene connectivity, and breath of expression in different tissues, sexes and life stages. This allows us both to disentangle the effect of pleiotropy from that of its covariates, and to assess the relative effect of antagonism between sexes, life stages, tissues and gene networks on the direction, strength, and efficacy of selection.

Results

A total of 10,631 and 9,895 genes were analyzed at coding and noncoding (untranslated regions [UTRs]) sites, respectively. The proportion of substitutions fixed by positive selection (α) was calculated based on the number of synonymous and nonsynonymous/UTRs polymorphic sites within *D. melanogaster* and divergent sites with *D. simulans* (see Materials and Methods). In the first two sections, we present results related to coding regions, whereas in the last section we compare them with noncoding regions.

General Modulators of Selection Efficacy

We first quantified the effect of factors that potentially affect the efficacy of selection by means of Spearman's rank correlations using binned data (fig. 1). We ranked genes by their value at each covariate and divided them into equally sized classes for numerical variables (see Materials and Methods); we then correlated the medians of the variable at each bin with the respective median α_{MK} values. As previously found (Campos et al. 2018; Charlesworth et al. 2018), we detected a faster-X effect, that is, a higher fraction of adaptive substitutions on X-linked genes compared with autosomal genes (medians: $\alpha_A = 0.600$, $\alpha_X = 0.817$; Wilcoxon's rank test: *P*-value = 2.94E-80, $n_A = 8{,}943$, $n_X = 1{,}688$; fig. 1*a*) and a faster rate of adaptive evolution (medians: $\omega A_A = 0.190$, $\omega A_X = 0.322$; Wilcoxon's rank test: *P*-value = 1.54E-49, $n_A = 8{,}943$, $n_X = 1{,}688$; supplementary fig. S2*a*, Supplementary Material online). This pattern held for all categories of sex-biased expression (male-biased: $\alpha_A = 0.800$ [$n_A = 799$], $\alpha_X = 0.831$ [$n_X = 90$], *P*-value = 3.43E-1; unbiased: $\alpha_A = 0.576$ [$n_A = 8{,}048$], $\alpha_X = 0.818$ [$n_X = 1{,}555$] *P*-value < 2.2E-16; female-biased: $\alpha_A = 0.548$ [$n_A = 96$], $\alpha_X = 0.746$ [$n_X = 43$], *P*-value = 0.224), which may indicate a primary role of the higher effective population size of the X compared with autosomes in *D. melanogaster* (see Campos et al. 2018 for a discussion).

We also found that the fraction of adaptive substitutions is strongly positively correlated with the recombination rate ($\rho = 0.932$, *P*-value = 8.02E-23, $n = 50$; fig. 1*b*), consistent with previous studies (Campos et al. 2014; Castellano et al. 2016). Similarly, there is a strong negative correlation between the length of the longest transcript and α ($\rho = -0.808$, *P*-value = 1.32E-12, $n = 50$; fig. 1*c*). We also confirmed earlier findings (Larracuente et al. 2008) that transcript length is negatively correlated with the evolutionary rate, *Dn*/*Ds* ($\rho = -0.962$, *P*-value = 8.38E-29, $n = 50$; supplementary fig. S2*c*, Supplementary Material online). These observations can be interpreted as a consequence of both positive and purifying selection at linked sites (Hill–Robertson interferences), between neighboring genes or between sites within a gene, which reduces the efficacy of selection in a linear manner (supplementary table S1, Supplementary Material online) in regions of low recombination and long genes.

Interestingly, we noted a strong decrease in the ratio of nonsynonymous to synonymous polymorphism, *Pn*/*Ps*, with the recombination rate ($\rho = -0.878$, *P*-value = 5.45E-17, $n = 50$; supplementary fig. S2*b*, Supplementary Material online), indicating that purifying selection is more efficient when interferences are weaker (see Campos et al. 2014 for similar results in noncrossover vs. crossover regions of *D. melanogaster*). On the contrary, the evolutionary rate, *Dn*/*Ds*, increased with recombination ($\rho = 0.608$, *P*-value = 2.89E-6, $n = 50$; supplementary fig. S2*b*), but the pattern was noisier. Previous analyses of the correlation between *Dn*/*Ds* and recombination have yielded mixed results (Betancourt and Presgraves 2002; Presgraves 2005; Zhang and Parsch 2005; Haddrill et al. 2007; Campos et al. 2014; Bolívar et al. 2016). This may reflect the fact that the predicted effect of recombination rate on *Dn*/*Ds* depends on the predominant mode of selection (and therefore on the set of genes used for the analysis): *Dn*/*Ds* is expected to be positively correlated with recombination under positive selection and negatively under purifying selection. The detection of a positive correlation supports a significant contribution of positive selection to protein divergence in *D. melanogaster* (consistent with the positive correlation between ωA and recombination: $\rho = 0.902$, *P*-value = 3.64E-19, $n = 50$; supplementary fig. S2*b*).

Genes with low expression are also known to be associated with increased rates of evolution, presumably because they are under relaxed purifying selection (e.g., Pál et al. 2006; Larracuente et al. 2008, see also our supplementary fig. S2*d*). However, the relationship between expression and the fraction of adaptive fixations is not as well understood (Carneiro et al. 2012). Figure 1*d* shows that the lower the expression level of a gene, the lower the fraction of adaptive fixations ($\rho = 0.551$, *P*-value = 3.41E-5, $n = 50$), whereas the rate of adaptive substitutions (ωA: $\rho = -0.773$, *P*-value = 4.67E-11, $n = 50$) and *Pn*/*Ps* ($\rho = -0.954$, *P*-value = 7.07E-27, $n = 50$) followed the opposite trend (supplementary fig. S2*d*). This suggests that genes with low expression are less conserved and evolve (adaptively) more rapidly than genes with higher expression. However, the relationship with α was nonlinear (Akaike information criterion: $AIC_{linear} = -131$, $AIC_{quadratic} = -172.3$, supplementary table S1) and mostly driven by very highly expressed genes that are under strong purifying selection but experience a higher adaptive evolutionary rate than expected linearly (supplementary fig. S2*d*).

Finally, α necessarily depends on the strength and frequency of positive selection itself. Genes under very strong constraint are expected to have low α, if their mutational space only includes very few beneficial mutations compared with neutral ones (supplementary fig. S2*e*). To account for this, we performed a supplementary analysis that incorporates *Dn*/*Ds* itself as a predictor (supplementary tables S3 and S4, Supplementary Material online). It should be noted that using *Dn*/*Ds* as a confounding variable is a conservative approach, as *Dn*/*Ds* and α are intrinsically correlated, leading to some loss of power to detect the effect of other predictors. However, it is an important control, especially when sex-biased genes, which are often under unusual selective regimes due to sexual selection, are considered.

Notably, all these patterns were robust to the different procedures used to filter the data (supplementary fig. S3*a*–*e*, Supplementary Material online): excluding singletons instead of variants below 5% frequency to control for slightly

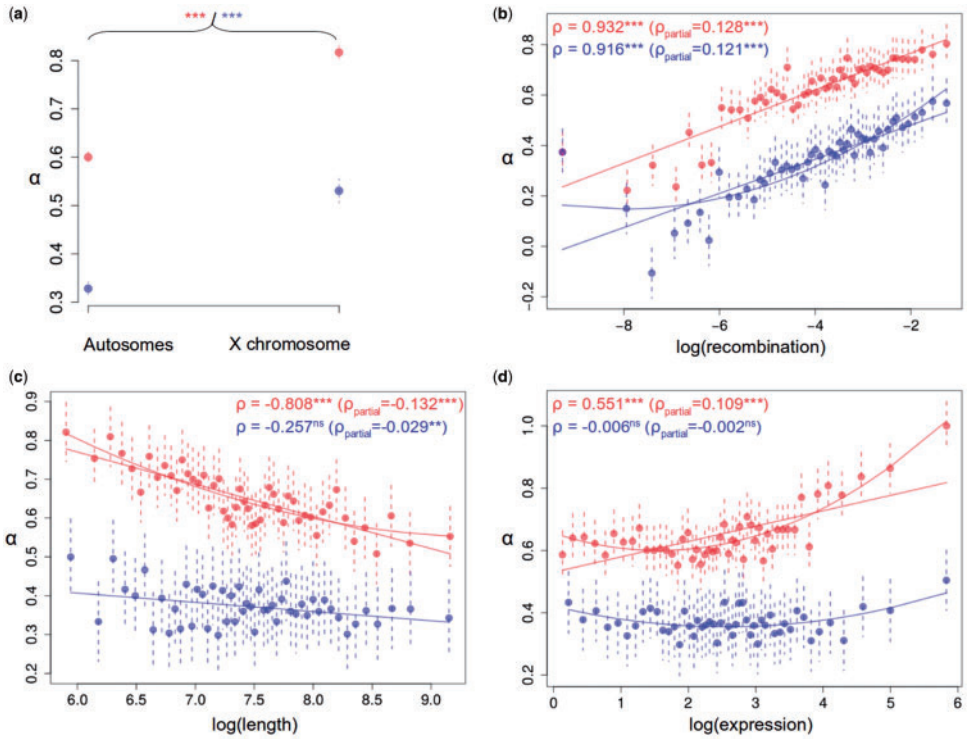

Fig. 1. The proportion of adaptive substitutions (α_{MK}) in coding (red) and noncoding (blue) regions is strongly influenced by general modulators. The relationship between each covariate (*x* axis) and α_{MK} (*y* axis) is shown in successive panels: (*a*) chromosomal location, (*b*) recombination rate (4**Ne***r* per bp), (*c*) length of the longest transcript (bp), and (*d*) global expression level (RPKM). Each point represents the median over genes grouped according to their values at each covariate. Error bars indicate 95% bootstrapped confidence intervals. For numerical covariates, the Spearman's rank correlation coefficient (ρ and $\rho_{partial}$) is given. Categorical covariates were compared with Wilcoxon's rank tests. Significance levels are denoted by asterisks (***$P < 0.001$, **$P < 0.01$, *$P < 0.5$, ns: non significant). The lines are least-squares regressions (linear or quadratic depending on which model best fitted the data based on AIC comparison; supplementary table S1, Supplementary Material online, for coding regions and supplementary table S2, Supplementary Material online, for noncoding regions), but they should be considered as indicative because of the binning procedure. Variants below 5% frequency were excluded.

deleterious polymorphisms; excluding transcript shorter than 900 bp to avoid small counts; and excluding X-linked genes, sex-biased genes, or immune genes as these factors have a strong effect on α (Obbard et al. 2009; Campos et al. 2018). Moreover, we estimated α with another method (Eyre-Walker and Keightley 2009) that explicitly models deleterious mutations based on the site frequency spectrum of all variants (supplementary fig. S2*a–e*, Supplementary Material online), and we again recovered all qualitative patterns.

The Proportion of Adaptive Substitutions under Different Pleiotropic Regimes

Our aim was to quantify the net effect of different facets of pleiotropy (namely, gene networks and breadth of expression across tissues, life stages, and sexes) on selection efficacy after controlling for the general modulators introduced above. This was done by applying Spearman's partial correlations on unbinned data (table 1*a*). Although partial correlations between α and the general modulators were weaker than correlations on binned data, they followed the same trends (fig. 1). In addition, we obtained partial correlations (supplementary table S3, Supplementary Material online) with the direction of selection (*DoS*) and the adaptive substitution rate (ωA_{MK}), and further estimated the effect size of each predictor in linear models (supplementary table S3, Supplementary Material online). Importantly, the general modulators alone explained 10.5% of the variance in *DoS* (respectively 9.5% for ωA_{MK}), whereas pleiotropy explained only 2.3% (respectively 2.5% for ωA_{MK}) of the total variance. The effect of all pleiotropic metrics combined was thus limited, but significant based on a likelihood ratio test (Log $L_{modulators}$ = 2,748.8, Log L_{all} = 2,893.2; *P*-value = 9.62E-58; supplementary table S3, Supplementary Material online). In comparison, the Hill–Robertson factors alone (recombination rate and transcript length) contributed up to 9.5% to the variance in *DoS* (respectively 7.9% for ωA_{MK}).

Gene Networks

Pleiotropy has been commonly measured by the number of interactions a gene is involved in, that is, gene connectivity. However, previous studies have found limited evidence of an effect of connectivity on evolutionary rate (e.g., *Dn*/*Ds*: Jordan et al. 2003; Hahn et al. 2004) or on the rate of adaptive substitutions (ωA: Josephs et al. 2017). Here, we investigated gene networks at four different levels (Murali et al. 2011): genetic interactions, that is, the modification of the phenotype of a mutant by an allele at a second gene; microRNA–gene interactions, predicted primarily from the

Table 1. Spearman's Rank Partial Correlations on α_{MK} in (*a*) Coding and (*b*) Noncoding Regions.

	(*a*) Coding		(*b*) Noncoding	
Covariate	**Estimate**	***P*-value**	**Estimate**	***P*-value**
Log(*recombination rate*)	**1.28E-001**	**6.61E-040*** **	**1.21E-001**	**1.86E-033*** **
Log(*transcript length*)	**−1.32E-001**	**1.55E-042*** **	**−2.89E-002**	**4.04E-003** **
Log(*expression level*)	**1.09E-001**	**2.76E-029*** **	**−2.01E-003**	**8.42E-001ns**
X chromosome	**1.31E-001**	**1.34E-041*** **	**7.78E-002**	**9.33E-015*** **
Gene–gene interactions	**2.57E-002**	**8.12E-003** **	**−2.39E-003**	**8.12E-001ns**
Protein–protein interactions	**4.03E-002**	**3.21E-005*** **	**9.12E-003**	**3.65E-001ns**
microRNA–gene interactions	**2.41E-003**	**8.04E-001ns**	**−3.66E-002**	**2.71E-004*** **
TF–gene interactions	**−9.08E-003**	**3.50E-001ns**	**1.02E-002**	**3.10E-001ns**
Sexually antagonistic genes	**−1.26E-002**	**1.93E-001ns**	**−2.99E-002**	**2.91E-003** **
Intersexual genetic correlation	**−1.90E-002**	**5.01E-002***	**6.69E-003**	**5.06E-001ns**
Folded sex specificity	**8.99E-002**	**1.72E-020*** **	**2.78E-002**	**5.79E-003** **
Tissue-by-stage specificity	**−6.68E-003**	**4.91E-001ns**	**−5.99E-003**	**5.52E-001ns**

Note.—Variants below 5% frequency were excluded.
Significance levels are denoted by asterisks: ***$P < 0.001$, **$P < 0.01$, *$P < 0.05$. ns: non significant.

complementarity of microRNAs and putative target genes; and experimentally derived transcription factor (TF)–gene interactions and protein–protein interactions. In all cases, there was a small number of highly connected genes (hubs), whereas the majority of the genes were involved in no or a few interactions. This pattern was extreme for genetic and protein–protein networks, where 88% and 71% of the genes had no interactors recorded, respectively, and only 10% and 6% displayed more than one interactor. Gene networks at the microRNA and TF levels were less skewed, with only 16% and 10% of the genes without interactors, respectively, and 10% and 26% showing more than 20 interactors.

If antagonistic molecular pleiotropy were widespread, genes with more interactors should have lower α values. Contrary to this, the most consistent pattern was a positive correlation between the number of protein–protein interactions and α ($\rho = 0.748$, *P*-value = 7.35E-3, $n = 12$; fig. 2*a*; $\rho_{partial} = 0.0403$, *P*-value = 3.21E-5, $n = 10{,}631$; table 1*a*), whereas patterns were not consistent across the different data sets for the other types of interactions (supplementary fig. S3*f*, Supplementary Material online). Accordingly, a stepwise selection approach showed that of the four measures of gene networks, only protein–protein interactions were relevant in the *DoS* (table 2*a*) and ωA (table 3*a*) linear models. In the case of microRNAs, an apparent negative correlation was observed between the number of interactions and α values ($\rho = -0.673$, *P*-value = 3.12E-4, $n = 24$; fig. 2*a*). However, this correlation was not significant with the alternative method of Eyre-Walker and Keightley (2009) (supplementary fig. S2*g*, Supplementary Material online), and disappeared when other covariates were accounted for ($\rho_{partial} = 2.41E\text{-}3$, *P*-value = 8.04E-1, $n = 10{,}631$; table 1*a*). This seemed to be partly due to the positive correlation between the number of microRNA–gene interactions and transcript length ($\rho = 0.368$, *P*-value < 2.2E-16, $n = 10{,}631$, supplementary fig. S1*a*, Supplementary Material online), which may be explained by the fact that many microRNA–gene interactions were estimated in silico based on sequence complementarity (and longer sequences have a higher chance of being complementary). Finally, supplementary fig. S2*f*, Supplementary Material online, indicates that the positive relationship between connectivity at the protein level and the fraction of adaptive fixations was mainly driven by stronger purifying selection acting on highly connected genes (*Pn/Ps*: $\rho = -0.863$, *P*-value = 2.99E-4, $n = 12$), whereas positive selection had a negligible effect (ωA: $\rho = -0.657$, *P*-value = 2.40E-2, $n = 12$). Taken together, these results suggest that the common assumption that highly connected genes are more likely to be under antagonistic molecular pleiotropy (Promislow 2004) may be unfounded (He and Zhang 2006).

Specificity of Expression across Tissues and Life Stages

Analyses of the effect of expression specificity on evolutionary rate have essentially been limited to adult tissues (Duret and Mouchiroud 2000; Grath and Parsch 2012), whereas other studies have found an impact of the timing of expression during development (early vs. late, e.g., Artieri et al. 2009) but did not survey its breadth across stages. Here, we explored the influence on α of expression specificity across: 1) four developmental stages ("stage specificity," supplementary fig. S3*j*, Supplementary Material online); 2) several tissues within each stage ("larval tissue specificity," "pupae tissue specificity," and "somatic adult tissue specificity," supplementary fig. S3*k*, Supplementary Material online); and 3) by combining these two dimensions ("tissue-by-stage specificity," supplementary fig. S3*l*, Supplementary Material online). As expected, we found that genes specifically expressed in a particular tissue and/or stage have low expression overall (ρ ranging from −0.461 to −0.586, and *P*-value < 2.2E-16 in all cases, $n = 10{,}631$, supplementary fig. S1*a*, Supplementary Material online). Interestingly, we also found a significant negative correlation between the number of TF interactions and the extent of expression specificity (ρ ranging from −0.415 to −0.662, and *P*-value < 2.2E-16, $n = 10{,}631$ in all cases, supplementary fig. S1*a*, Supplementary Material online), suggesting that broadly expressed genes have a more complex regulatory architecture. As there was a positive correlation between the five "expression specificity" metrics (ρ ranging from 0.493 to 0.932, and *P*-value < 2.2E-16, $n = 10{,}631$ in all cases, supplementary fig. S1*a*, Supplementary Material

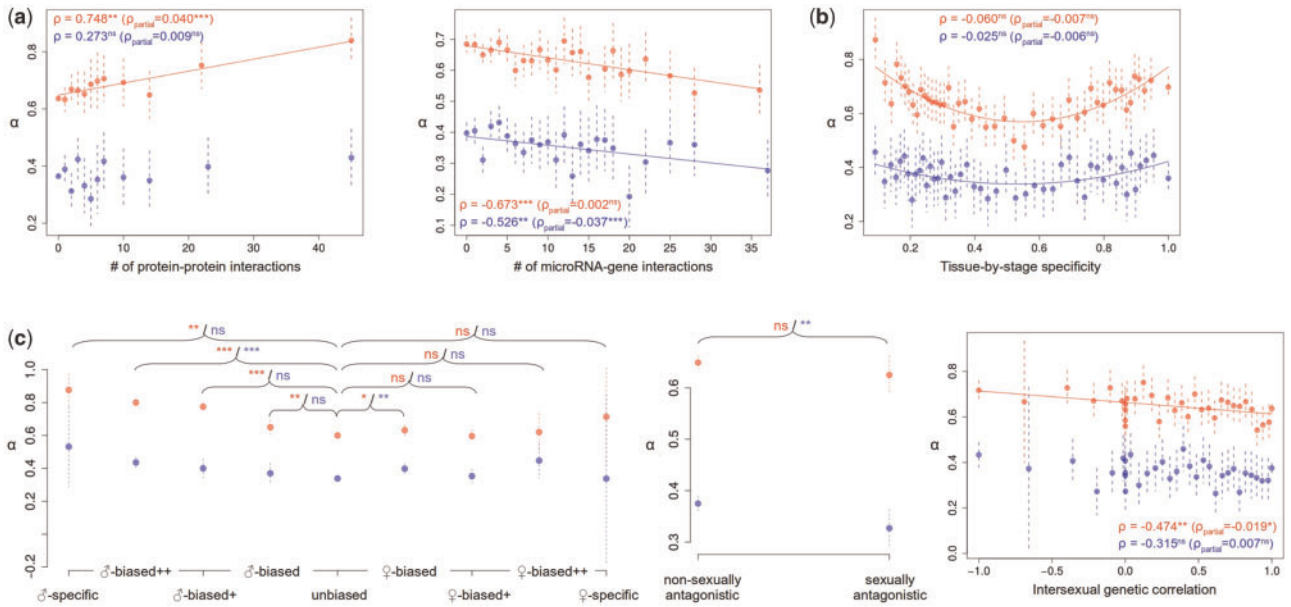

Fig. 2. The proportion of adaptive substitutions (α_{MK}) in coding (red) and noncoding (blue) regions is moderately influenced by different facets of pleiotropy: (*a*) gene networks: protein–protein interactions and microRNA–gene interactions, (*b*) tissue-by-stage specificity, and (*c*) sex-related metrics: sex specificity, sexual antagonism, and intersexual genetic correlation. Other details match figure 1.

Table 2. Best Linear Model on *DoS* Obtained After a Stepwise Model Selection in (*a*) Coding and (*b*) Noncoding Regions.

	(*a*) Coding		(*b*) Noncoding	
Covariate	**Estimate**	***P*-value**	**Estimate**	***P*-value**
Intercept	**1.41E-001**	**0.00E+000*** **	**6.78E-002**	**2.53E-250*** **
Log(*recombination rate*)	**3.71E-002**	**1.71E-079*** **	**2.53E-002**	**1.92E-042*** **
Log(*transcript length*)	**−3.38E-002**	**8.28E-069*** **	**−1.64E-002**	**8.99E-017*** **
Log(*expression level*)	**−3.54E-003**	**1.05E-001ns**	**5.20E-003**	**1.19E-002***
X chromosome	**5.60E-002**	**4.80E-026*** **	**4.90E-002**	**8.94E-023*** **
Gene–gene interactions				
Protein–protein interactions	**2.80E-003**	**1.34E-001ns**	**4.36E-003**	**1.38E-002***
microRNA–gene interactions			**4.06E-003**	**2.99E-002***
TF–gene interactions				
Sexually antagonistic genes			**−1.40E-002**	**1.53E-002***
Intersexual genetic correlation				
Folded sex specificity	**2.87E-002**	**1.66E-051*** **	**5.37E-003**	**3.15E-003** **
Tissue-by-stage specificity	**7.10E-003**	**2.69E-003** **	**−4.23E-003**	**6.03E-002ns**

Note.—Shaded cells show the discarded covariates. Variants below 5% frequency were excluded.
Significance levels are denoted by asterisks: ***$P < 0.001$, **$P < 0.01$, *$P < 0.05$. non significant.

online), and they were redundant in a principal component analysis (supplementary fig. S1*b*, Supplementary Material online), we focused only on the combined measure across tissues and stages (tissue-by-stage specificity) to avoid collinearity issues.

The relationship between α and tissue-by-stage specificity (fig. 2*b*) was significantly better explained by a quadratic model than a linear model ($AIC_{linear} = -107.6$, $AIC_{quadratic} = -149.1$, supplementary table S1, Supplementary Material online), and this pattern was consistent across the different data sets (supplementary fig. S3*l*, Supplementary Material online) and methods (supplementary fig. S2*k*, Supplementary Material online). Accordingly, the Spearman's correlation could not capture this nonmonotonic trend ($\rho = -0.0596$, *P*-value = 0.691, $n = 47$, fig. 2*b*; $\rho_{partial} = -0.007$, *P*-value = 0.491, $n = 10{,}631$, table 1*a*). Supplementary fig. S2*k*, Supplementary Material online, reveals that the "U-shaped" pattern arises from the combination of a negative linear relationship between expression specificity and the strength of purifying selection (either using the fraction of strongly deleterious mutations [$\rho = -0.890$, *P*-value < 2.2E-16] or *Pn/Ps* [$\rho = 0.948$, *P*-value = 6.46E-24, $n = 47$] as found by Huber et al. 2017) and a positive nonlinear relationship with the adaptive evolutionary rate (ωA, $\rho = 0.672$, *P*-value = 2.32E-7, $n = 47$). This suggests that an increased fraction of adaptive substitutions can be either caused by strong purifying selection on highly

Table 3. Best Linear Model on ωA_{MK} Obtained After a Stepwise Model Selection in (*a*) Coding and (*b*) Noncoding Regions.

	(*a*) Coding		(*b*) Noncoding	
Covariate	**Estimate**	***P*-value**	**Estimate**	***P*-value**
Intercept	3.60E-001	0.00E+000***	2.43E-001	9.66E-049***
Log(*recombination rate*)	1.12E-001	1.05E-043***	1.23E-001	3.94E-015***
Log(*transcript length*)	−1.42E-001	1.10E-070***	−1.21E-001	3.23E-013***
Log(*expression level*)	−6.94E-002	1.45E-014***	−2.45E-002	1.53E-001ns
X chromosome	1.65E-001	4.81E-014***	1.82E-001	1.51E-005***
Gene–gene interactions				
Protein–protein interactions	1.39E-002	7.15E-002ns		
MicroRNA–gene interactions			2.74E-002	8.12E-002ns
TF–gene interactions				
Sexually antagonistic genes			−8.72E-002	7.25E-002ns
Intersexual genetic correlation			2.71E-002	6.29E-002ns
Folded sex specificity	1.11E-001	6.04E-046***		
Tissue-by-stage specificity	4.73E-002	1.30E-006***	−3.72E-002	3.95E-002*

NOTE.—Shaded cells show the discarded covariates. Variants below 5% frequency were excluded.
Significance levels are denoted by asterisks: ***$P < 0.001$, **$P < 0.01$, *$P < 0.05$. ns: non significant.

pleiotropic genes (i.e., broadly expressed) or enhanced positive selection on weakly pleiotropic genes (i.e., specifically expressed).

Sex-Biased Genes and Sexual Antagonism

As others have recently found (Avila et al. 2015; Campos et al. 2018), male-biased genes are characterized by a higher proportion of adaptive substitutions than unbiased genes but not female-biased genes, leading to an asymmetric "U-shaped" pattern (fig. 2*c*). This pattern, observed based on whole-body samples and robust to varying data sets (supplementary fig. S3*g*, Supplementary Material online) and methods (supplementary fig. S2*h*, Supplementary Material online), was mostly driven by reproductive tissues; heads did not show sufficient sexual dimorphism for such an analysis to be meaningful (supplementary fig. S4, Supplementary Material online). When merging male-biased and female-biased genes together, the folded sex specificity had a significant positive effect on α after controlling for other factors ($\rho_{partial} = 0.0899$, *P*-value = 1.72E-20, $n = 10{,}631$, table 1*a*). It was also retained in the best linear regression on *DoS* (table 2*a*) and ωA (table 3*a*), confirming its influence on selection.

Several hypotheses have been put forward to explain this accelerated evolution of male-biased genes. First, the fact that adaptive evolution is stronger in male-biased genes than in unbiased and female-biased genes, and that male-biased genes are primarily expressed in the male reproductive organs (supplementary fig. S5, Supplementary Material online), may indicate that sexual selection originating from male–male competition drives this pattern. However, male sexual selection is unlikely to be the only process at play, because male-biased genes had a consistently higher fraction of adaptive fixations than unbiased and female-biased genes across three categories of evolutionary rate ("slow," "intermediate," and "fast" evolving genes; supplementary fig. S6, Supplementary Material online). Similarly, partial correlations show that sex bias remains a strong predictor of α even when *Dn*/*Ds* is corrected for ($\rho_{partial} = 0.0584$, *P*-value = 1.72E-9, $n = 10{,}631$; supplementary table S3, Supplementary Material online).

Second, sexual antagonistic pleiotropy could produce a similar "U-shaped" pattern as genes under sexual antagonism will exhibit unbiased expression, whereas intrasexual conflict is expected to be resolved by sex-specific expression. We took two approaches to detect an effect of sexual conflict on selection. First, we estimated α for a set of genes that had experimentally been detected as sexually antagonistic (Innocenti and Morrow 2010). The median folded sex specificity was 0.807 for sexually antagonistic genes, and 1.00 for nonsexually antagonistic ones (Wilcoxon's rank test: *P*-value = 2.5E-11, $n_{SAG} = 1{,}009$, $n_{SAG} = 9{,}622$), as expected if dimorphism provides a resolution of conflict. However, when we compared α between the two sets of genes, we did not find any significant difference (medians: $\alpha_{SAG} = 0.625$, $\alpha_{non\text{-}SAG} = 0.649$; Wilcoxon's rank test: *P*-value = 0.354, $n_{SAG} = 1{,}009$, $n_{non\text{-}SAG} = 9{,}622$; fig. 2*c*), and this was consistent across data sets (supplementary fig. S3*h*, Supplementary Material online, except when excluding only singletons) and methods (supplementary figs. S2*i* and S7, Supplementary Material online). As genes were classified as sexually antagonistic based on interactions between expression and sex-specific fitness (Innocenti and Morrow 2010), selection at the coding sequence level may not be involved in the conflict. A second approach was to look at the intersexual correlation of expression of each gene, which is thought to underlie much of the sexual conflict (as it prevents the two sexes from reaching their optimum; Dean and Mank 2016). The intersexual genetic correlation in expression (which was negatively correlated to folded sex specificity, $\rho = -0.185$, *P*-value < 2.2E-16, $n = 10{,}631$, supplementary fig. S1*a*, Supplementary Material online; see Griffin et al. 2013 and Allen et al. 2018 for similar results) was negatively correlated with α ($\rho = -0.474$, *P*-value = 5.36E-003, $n = 33$, fig. 2*c*; $\rho_{partial} = -0.019$, *P*-value = 5.01E-2, $n = 10{,}631$, table 1*a*), confirming that part of these highly correlated genes may be under sexual conflict. Although the trend was consistent across data sets (supplementary fig. S3*i*, Supplementary Material online), it was not significant with

the Eyre-Walker and Keightley method (supplementary fig. S2*j*, Supplementary Material online).

Third, male-biased genes are more tissue-specific than other genes (e.g., in *Drosophila*: Meisel 2011; Grath and Parsch 2012; in vertebrates: Mank et al. 2008), and their increased α may be mainly driven by tissue specificity. Consistent with this, we found a significant positive correlation between the folded sex specificity and the adult tissue specificity calculated including male and female reproductive tissues ($\rho = 0.200$, *P*-value < 2.2E-16), confirming previous findings in *Drosophila* (Assis et al. 2012; Allen et al. 2018). Disentangling the effect of tissue specificity is difficult because reproductive genes have by far the most specific patterns of expression of any tissue (64% of all fully adult tissue-specific genes were expressed in the male reproductive tissues). In order to get around this, we focused instead on all genes with high expression in the male reproductive tissues (testis and accessory glands), and divided those into three categories of adult tissue specificity: broad ($\tau < 0.4$; 952 genes), intermediate ($0.4 \leq \tau \leq 0.8$; 273 genes), and specific ($\tau > 0.8$; 946 genes). Supplementary figure S8, Supplementary Material online, shows that the two extreme categories have similarly high α values (medians: $\alpha_{broad} = 0.833$, $\alpha_{intermediate} = 0.730$, and $\alpha_{specific} = 0.804$, respectively), suggesting that tissue specificity is not the primary cause of increased selection efficacy of male-biased genes (Meisel 2011; Grath and Parsch 2012).

Finally, the fact that female-biased genes were not significantly different from unbiased genes in terms of α (fig. 2*c*) may be due to their higher breadth of expression (e.g., only 13 genes were strictly expressed in female reproductive tissues). In particular, female-biased genes were far more expressed in the carcass and digestive systems of adults than male-biased genes (supplementary fig. S5, Supplementary Material online). Moreover, female-biased genes were highly expressed in the embryo (supplementary fig. S5, Supplementary Material online), suggesting that many of them function as maternal RNAs, which should further constrain their evolutionary dynamics due to ontogenic pleiotropy.

The Efficacy of Selection at Coding and Noncoding Sites

We compared the selective regime of coding sequences and the UTRs of transcripts, which are known to be involved in gene regulation (Barrett et al. 2012). Synonymous sites were used as the neutral control for both analyses, whereas in the analysis of noncoding regions *Du* and *Pu* refer to mutations in the UTRs. Overall, the median fraction of adaptive substitutions was higher in coding than noncoding regions ($\alpha_{coding} =$ 64.6% vs. $\alpha_{noncoding} = 36.7\%$; Wilcoxon's rank test: *P*-value < 2.2E-16, $n_{coding} = 10{,}631$, $n_{noncoding} = 9{,}895$), and these values were close to those previously reported (Andolfatto 2005). Although the divergence ratio was slightly lower in coding regions ($Dn/Ds_{coding} = 40\%$ vs. $Du/Ds_{noncoding} = 49\%$; Wilcoxon's rank test: *P*-value < 2.2E-16, $n_{coding} = 10{,}631$, $n_{noncoding} = 9{,}895$), there was a 2-fold decrease in the median polymorphism ratio in coding regions compared with noncoding regions ($Pn/Ps_{coding} = 16\%$ vs. $Pu/Ps_{noncoding} = 32\%$ when excluding variants below 5% frequency; Wilcoxon's rank test: *P*-value < 2.2E-16, $n_{coding} = 10{,}631$, $n_{noncoding} = 9{,}895$), confirming previous findings that the latter are less constrained (Campos et al. 2018). At the genome level, α values in coding and noncoding regions were moderately but significantly correlated ($\rho = 0.23$, *P*-value < 2.2E-16, $n = 9{,}895$), suggesting that the selective pressures acting on genes and on their regulatory sequences are comparable.

Consistent with this, most strong modulators of selection had similar effects on α for coding and noncoding sequences (we obtained comparable patterns with *DoS* and ωA, supplementary table S4, Supplementary Material online). Corroborating results by Campos et al. (2018), we found a strong faster-X effect in UTRs (medians: $\alpha_A = 0.328$, $\alpha_X = 0.530$; Wilcoxon's rank test: *P*-value = 6.28E-41, $n_A = 8{,}299$, $n_X = 1{,}596$; fig. 1*a*), consistent with faster gene expression divergence on the X chromosome compared with the autosomes (Kayserili et al. 2012; Meisel et al. 2012). Moreover, selection efficacy strongly increased with the local recombination rate ($\rho = 0.916$, *P*-value = 1.19E-20, $n = 50$, fig. 1*b*; $\rho_{partial} = 0.121$, *P*-value = 1.86E-33, $n = 9{,}895$, table 1*b*). We also found a significant negative partial correlation between the length of the transcript and selection efficacy on its UTRs ($\rho_{partial} = -0.029$, *P*-value = 4.04E-3, $n = 9{,}895$, table 1*b*). However, there was no linear effect of expression level of the transcript on selection efficacy on its UTRs ($\rho = -0.006$, *P*-value = 0.968, $n = 50$, fig. 1*d*; $\rho_{partial} = -0.002$, *P*-value = 0.842, $n = 9{,}895$, table 1*b*). This may reflect the fact that, contrary to what is observed for amino acid divergence, the rate of adaptive divergence of gene expression appears to be reduced for high expression genes (Nourmohammad et al. 2017). Taking into consideration general modulators alone, 4.9% of the variance in *DoS* (respectively 1.6% for ωA) was explained (supplementary table S4, Supplementary Material online), which is lower than in coding sequences (supplementary table S3, Supplementary Material online), as modulators were mostly designed based on coding information.

Similarly, the effect of all pleiotropic metrics combined was lower to that found in coding regions (*DoS*: 0.2%; ωA: 0.1%) but was significant based on a likelihood ratio test (Log $L_{modulators} = 3{,}574.0$, Log $L_{all} = 3{,}589.7$; *P*-value = 2.71E-4; supplementary table S4, Supplementary Material online). Patterns obtained for gene networks were qualitatively similar to those obtained using coding sequences. First, there was a positive correlation between α and the number of protein–protein interactions, but it was not significant for noncoding regions ($\rho = 0.273$, *P*-value = 0.391, $n = 12$, fig. 2*a*; $\rho_{partial} = 0.009$, *P*-value = 0.365, $n = 9{,}895$, table 1*b*). We also found a negative correlation between α and the number of microRNA–gene interactions ($\rho = -0.526$, *P*-value = 8.32E-3, $n = 24$, fig. 2*a*). Contrary to coding regions, this negative correlation remained significant after controlling for other factors ($\rho_{partial} = -0.037$, *P*-value = 2.7E-4, $n = 9{,}895$, table 1*b*), and after the stepwise model selection on *DoS* (table 2*b*), which may reflect the fact that microRNAs bind primarily to 3′-UTRs. We also found the same "U-shaped" pattern (fig. 2*b*) in the relation between the fraction of adaptive fixations and the tissue-by-stage specificity

($AIC_{linear} = -142.9$, $AIC_{quadratic} = -150.6$, supplementary table S2, Supplementary Material online).

Estimates of sexual antagonism pleiotropy were also correlated with α for noncoding regions. A positive correlation between sex specificity and α was comparable but weaker to that of coding regions (fig. 2*c*; folded sex specificity: $\rho_{partial} = 0.0277$, *P*-value = 5.80E-8, $n = 9{,}895$, table 1*b*). The same was true for the intersexual genetic correlation in expression ($\rho = -0.315$, *P*-value = 7.4E-2, $n = 33$, fig. 2*c*), which was nonsignificant after accounting for other factors ($\rho_{partial} = 0.006$, *P*-value = 5.06E-1, $n = 9{,}895$, table 1*b*). On the contrary, the pattern was stronger in noncoding regions when considering genes that were previously classified as sexually antagonistic based on expression data (Innocenti and Morrow 2010 and see Materials and Methods). Sexually antagonistic genes were under less efficient selection compared with other genes ($\alpha_{SAG} = 0.327$, $\alpha_{non\text{-}SAG} = 0.375$; Wilcoxon's rank test: *P*-value = 5.20E-3, $n_{SAG} = 954$, $n_{non\text{-}SAG} = 954$; fig. 2*c*), as expected if opposing selective forces are acting on male and female expression. Moreover, sexual antagonism was retained in the best model after stepwise selection on *DoS* (table 2*b*) and on ωA (table 3*b*).

Discussion

Pleiotropy is predicted to restrict the efficacy of selection, because trade-offs between mutations that benefit one biological process but harm others are more likely to occur in pleiotropic genes. There has been substantial debate in the literature about the effect of pleiotropy on evolutionary rates, and to a lesser extent, on selection efficacy. In this study, we shed light on the factors influencing selection efficacy in *D. melanogaster* and disentangle the relative contribution of different aspects of pleiotropy from that of these confounding factors. Correlates are rarely accounted for in similar studies and may have led to an overestimate of the effect of pleiotropy. We explain 4.9% of the variance in the direction of selection (*DoS*) (respectively 6.3% for ωA) when only considering pleiotropic metrics. When general modulators are taken into account (chromosomal location, Hill–Robertson effects, expression level), the eight pleiotropic metrics (molecular interactions, sex-related metrics, tissue-by-stage specificity) have a significant but relatively small effect on selection efficacy in coding regions: 2.3% of the total variance in *DoS*, whereas the two Hill–Robertson factors alone explain up to 9.5% and the complete model 12.8% (respectively 2.5%, 7.9%, and 12.0% for ωA). These estimates should be taken with some caution because of several caveats in the analysis. First, the method assumes a linear relationship between *DoS* and each predictor, which is clearly not the case with some pleiotropic metrics, such as tissue-by-stage specificity. Second, the different data sets employed come from different populations of *D. melanogaster*, and biological differences between them could have affected our results. African populations were used for the genomic data (Zambia) and for the recombination estimates (Rwanda), whereas American flies were used to identifying the sexual antagonistic genes (LH_m lab strain), for the intersexual genetic correlations (Raleigh), and for the expression data (modENCODE: Oregon-R and ISO1). Some studies have reported a fair amount of divergence among populations in the magnitude of sex-bias (e.g., in *D. melanogaster*: Huylmans and Parsch 2014; in *D. serrata*: Allen et al. 2017; but see Müller et al. 2012 for a counterexample). However, we expect that these differences would add noise in our data, therefore making our conclusions conservative. Finally, we used synonymous sites as our neutral control, although these have been shown to be under purifying selection in *D. melanogaster*, especially when highly expressed genes are considered (Lawrie et al. 2013). The extreme values of α and ωA that we observed for genes with the highest expression (supplementary fig. S2*d*, Supplementary Material online) may therefore partly be due to the strong purifying selection acting on synonymous sites, which can bias α upwards (Matsumoto et al. 2016). Despite these limitations, our results generally support the idea that the adaptive potential of a gene that has either multiple molecular functions or is expressed in multiple contexts (sexes, life stages, tissues) may be to some degree restricted.

Different aspects of pleiotropy appear to restrict adaptation to different extents. First, the influence of gene connectivity on α was not robust to filtering choices or methodologies at any of the four levels investigated, and highly connected genes did not appear to be under less effective selection. Previous work has primarily focused on purifying selection, and conclusions have also been inconsistent (Jordan et al. 2003; Hahn et al. 2004; Hahn and Kern 2005; Larracuente et al. 2008). Similarly, functional analyses in which the number of biological processes of a gene was recorded found limited effects of molecular pleiotropy on the evolutionary rate in yeasts (Salathé et al. 2006), and on α or ωA in coexpression networks in plants (Josephs et al. 2017). Finally, an RNAi study performed in *D. melanogaster* (Vedanayagam and Garrigan 2015) found that more pleiotropic genes, that is, those having a measurable effect on multiple molecular phenotypes, are in fact under stronger positive selection. Collectively, these findings suggest that gene connectivity, despite having been widely used, is not an accurate indicator of antagonistic molecular pleiotropy (He and Zhang 2006).

On the other hand, we detected an influence of sex specificity on selection efficacy. Our results suggested that this was not solely driven by the fast evolution of male-biased genes due to sexual selection, nor by their strong tissue specificity. We argue that sex specificity may be an efficient way to escape pleiotropic sexual antagonism and to evolve toward optimal sex-specific phenotypes. A caveat concerning this reasoning is our assumption that sex-biased genes typically have sex-biased fitness effects. Empirical tests are scarce but found that this is generally true in *D. melanogaster* (Connallon and Clark 2011). Finally, several studies have considered the effect of tissue specificity on the overall evolutionary rate (*Dn*/*Ds*) and found a positive correlation (Duret and Mouchiroud 2000; Larracuente et al. 2008), suggesting that adaptation is more prevalent in the absence of tissue pleiotropy. Likewise, breadth of expression across developmental stages may impede selection efficacy, especially in holometabolous insects,

as it has been reported in *D. melanogaster* (Perry et al. 2014). A notable finding of our work is that by combining both the temporal (life stages) and spatial (tissues) dimensions, an intermediate level of tissue-by-stage specificity appears to lead to maladaptation. We suggest that this complex pattern arises because the accumulation of slightly deleterious nonsynonymous fixations is not compensated by adaptive fixations for intermediate level of ontogenic pleiotropy.

Our estimate of α in coding regions was above 50%, consistent with what has been found in *Drosophila* (Andolfatto 2005; Eyre-Walker et al. 2006) and in other animal species (Galtier 2016). This value was ~35% for noncoding regions (UTRs), which is similar to the 37.1% reported by Andolfatto (2005). These results confirm that these sequences are under effective natural selection (Andolfatto 2005; Elyashiv et al. 2016; Campos et al. 2017), supporting their role in the regulation of gene expression (Barrett et al. 2012). We found that pleiotropy has similar consequences on selection efficacy for mutations in coding regions and for those regulating gene expression, though effects were generally less pronounced in the latter. Notably, we found more support for an influence of sex-specific selection on regulatory evolution than previously reported. We observed an asymmetric U-shaped pattern between sex specificity and α in noncoding regions, contrary to Campos et al. (2018), who did not find faster adaptive evolution of male-biased genes in UTRs. The reason for this discrepancy is not entirely clear, but may have to do with how genes were classified in sex-bias categories, as Campos et al. (2018) employed a more sophisticated method. Genes that had been detected as having sexually antagonistic effects on fitness (Innocenti and Morrow 2010) also had reduced α values, further supporting the role of sexual conflict in limiting the efficacy of selection on regulatory regions.

Although our results were robust to different .filtering procedures and methods to estimate α, the weak effects reported may be partly due to incomplete information on pleiotropy. There are many conflicting definitions of pleiotropy (Paaby and Rockman 2013), and many ways of estimating it. Some studies (Salathé et al. 2006; McGuigan et al. 2014) have used the number of annotated gene ontology terms, but concluded a weak effect on the rate of evolution or on the strength of stabilizing selection; this was the case even when pleiotropy within functional modules (modular pleiotropy) was considered (Collet et al. 2018). More direct and accurate measures include quantitative trait locus mapping (e.g., in mice, Wagner et al. 2008) and RNAi screening (e.g., in yeast, Ohya et al. 2005). These studies have shown that most of the genes influence only a few phenotypes (L-shaped distribution of pleiotropy, Wagner and Zhang 2011; but see Hill and Zhang [2012] for a counterpoint), but how applicable this is to other organisms is still unclear. Overall, our knowledge of the consequences of pleiotropy is still scarce, and thus future empirical studies should focus on what matters from an evolutionary perspective, that is, when a single gene influences more than one fitness component.

Materials and Methods

Genomic Data

Polymorphism within D. melanogaster

We used the *Drosophila* Population Genomics Project phase 3 data (Lack et al. 2015) consisting of a sample of 197 haploid genomes from a single locality, Siavonga in Zambia (Africa). This locality is considered to be part of the ancestral range for the species (Pool et al. 2012), and so the population shows high genetic diversity and has a simple demography. Whole-genome data for chromosome 2 (arms 2R and 2L), chromosome 3 (arms 3R and 3L) and chromosome X were retrieved from the Pool lab (http://johnpool.net/genomes.html, "DPGP3 SEQ" downloaded in September 2017). We sequentially masked regions with evidence of 1) heterozygosity, 2) identity by descent, and 3) admixture from non-African populations using the "MASKING PACKAGE" provided by the Pool lab. We then converted the 197 haploid sequences to standard vcf format using snp-sites.v2.3.3 (Page et al. 2016) and the *D. melanogaster* release 5.57 genome (http://popfly.uab.cat) as the reference. We filtered-out sites with more than 50% missing data with VCFtools v0.1.12 (Danecek et al. 2011). The "ingroup vcf" (available in supplementary file S1, Supplementary Material online) provides a list of polymorphic sites segregating in the Zambia population.

Divergence with D. simulans

We retrieved the *D. simulans* 2 genome aligned to the *D. melanogaster* 5.57 genome from the Pool lab (http://johnpool.net/genomes.html, "SIMULANS SEQ" downloaded in September 2017). We then converted the *D. simulans* sequence to standard vcf format using snp-sites.v2.3.3 and the *D. melanogaster* release 5.57 genome as reference. Sites segregating within the Zambia population were discarded, so the "outgroup vcf" (available in supplementary file S2, Supplementary Material online) provides a list of divergent sites between *D. simulans* and *D. melanogaster*. Alleles at each site were orientated based on the *D. simulans* sequence (sites with missing data in *D. simulans* were discarded).

Annotation

Only biallelic sites were considered for further analyses, and only the longest transcript of each gene was retained. We conducted variant annotation based on the vcfs with SnpEff v4.3r (Cingolani et al. 2012) using the *D. melanogaster* BDGP5.75 database. For each transcript, we extracted the number of synonymous (tagged "synonymous_variant") and nonsynonymous (tagged "missense_variant") polymorphic sites (*Ps* and *Pn*, respectively) from the annotated "ingroup vcf". Similarly, we extracted the number of synonymous and nonsynonymous divergent sites (*Ds* and *Dn*, respectively) from the annotated "outgroup vcf". To investigate the evolution of noncoding DNA, we also extracted the number of UTR variants (tagged "3_prime_UTR_variant" and "5_prime_UTR_variant") as an alternative nonneutral class

of sites in the "ingroup" and "outgroup" vcfs (*Pu* and *Du*, respectively). Annotations for each transcript are provided in supplementary file S3, Supplementary Material online, for coding data and supplementary file S4, Supplementary Material online, for noncoding data.

In the Supplementary Material online, we performed an additional annotation based on vcfs with SNPGenie (Nelson et al. 2015) using the *D. melanogaster* 5.75 genome and annotation file (ftp.flybase.net/releases/FB2014_03/dmel_r5.57). SNPGenie was run twice: once for the forward strand with argument vcfformat = 1 and once for the complementary strand. For each transcript, we obtained the total number of potential synonymous and nonsynonymous sites (*Ns* and *Nn*, respectively), together with *Ps*, *Pn*, *Ds*, and *Dn* as described above. We also computed the folded synonymous and nonsynonymous site frequency spectra (*SFSs* and *SFSn*, respectively) by downsampling 186 haplotypes at each site to get data without missing genotypes. Annotations for each transcript are provided in supplementary file S5, Supplementary Material online.

Expression Data

We used the Model Organism ENCyclopedia Of Dna Elements (modENCODE Consortium 2010) that provides RNA-seq expression patterns in *D. melanogaster* across multiple developmental stages (embryos, larvae, pupae, male and female adults) and types of tissues (carcass, fat, salivary glands, digestive system, imaginal discs, central nervous system [CNS], heads, ovaries, testes, and accessory glands). The expression data ("gene_rpkm_report_fb_2017_04.tsv.gz") were retrieved from ftp.flybase.net/releases/current/precomputed_files/genes in October 2017. Expression values were provided as the number of reads per kilobase per million reads (RPKM) summed over all transcripts for each gene. We quantile normalized the expression values between samples using the R package "preprocessCore" v1.36.0 (Bolstad 2017). Normalization was applied either 1) between male and female adults, 2) between developmental stages for whole body samples, or 3) between tissues for a given developmental stage. In total, we had 56 samples across all tissues and developmental stages, among which three were removed due to very low expression after normalization ("em0.2hr," "L3_Wand_fat," and "L3_Wand_saliv" stages). No minimal expression cutoff was applied. Gene expression values for each sample are provided in supplementary file S6, Supplementary Material online.

Efficacy of Selection

The Proportion and Rate of Adaptive Substitutions: McDonald–Kreitman Method

Based on the SnpEff annotation, we calculated the proportion of nonneutral substitutions fixed by adaptation (α). High values of α can be due to either increased efficacy of positive selection (higher rate of fixation of adaptive substitutions) and/or increased efficacy of purifying selection (lower rate of fixation of deleterious substitutions). We compared the number of sites that were polymorphic within *D. melanogaster* and divergent between *D. melanogaster* and *D. simulans* for a selected class of sites (nonsynonymous or UTR variants) to a neutral reference (synonymous variants) as follows: $\alpha_{MK} = 1 - (Pn/Ps)/(Dn/Ds)$ (Smith and Eyre-Walker 2002, based on an extension of the McDonald–Kreitman test [McDonald and Kreitman 1991]). We assumed that synonymous variants are neutral. Although there is little evidence for current selection on codon usage bias in *D. melanogaster* (McVean and Vieira 2001), some purifying selection is likely acting on synonymous sites in high expression genes (Lawrie et al. 2013; see Discussion). We excluded rare variants from the analysis (below 5% frequency in our 197 haplotype sample), because the presence of slightly deleterious mutations segregating within species is expected to bias estimates of α downward (Fay et al. 2001, Charlesworth and Eyre-Walker 2008). Estimates were obtained for both coding (supplementary file S3, Supplementary Material online) and noncoding regions (supplementary file S4, Supplementary Material online). In the Supplementary Material online, we additionally obtained estimates of α_{MK} in coding regions by: 1) removing transcripts shorter than 900 bp; 2) excluding X-linked genes; 3) excluding sex-biased genes (SBR > -4 or SBR > 4); 4) excluding immune genes ($n = 483$ genes with GO:0002376 "immune system process" on http://flybase.org; last accessed October 2018); or 5) removing only singletons. Finally, from α_{MK} we deduced the rate of fixation of beneficial mutations relative to the rate for neutral mutations, as follows: $\omega A_{MK} = \alpha_{MK} * Dn/Ds$ (Muyle et al. 2018). This complementary metric is suitable under a nearly neutral regime as α_{MK} would be affected by the rate of both nonadaptive and adaptive substitutions.

The Proportion and Rate of Adaptive Substitutions: Eyre-Walker and Keightley Method

Based on the SNPGenie annotation and all variants, we alternatively calculated α with the approach of Eyre-Walker and Keightley (2009). The method is described in the appendix of their paper, and implemented in the software DoFEα (http://www.sussex.ac.uk/lifesci/eyre-walkerlab/resources; last accessed October 2017). This extension of the classic McDonald and Kreitman framework (1991) explicitly models the contribution of deleterious mutations to polymorphism and divergence, and corrects for distortions of the site frequency spectrum, either due to recent demographic changes or genetic draft (Messer and Petrov 2013), by introducing a series of nuisance parameters. The method uses the folded *SFSs*, folded *SFSn*, *Ns*, and *Nn* to infer the distribution of fitness effects (DFE) of new mutations by fitting a gamma distribution with two parameters (the shape and the mean strength of selection), based on the method of Eyre-Walker et al. (2006). From the DFE, the method calculates the proportion of mutations in four ranges of *Ne*s*, where *Ne* is the effective population size and *s* is the selection coefficient for deleterious mutations in heterozygotes: 1) *Ne*s* = 0–1 (nearly neutral); 2) *Ne*s* = 1–10; 3) *Ne*s* = 10–100; and 4) *Ne*s* > 100 (strongly deleterious). We also calculated the rate of adaptive substitution relative to neutral (ωA_{EWK}) following the method of Gossmann et al. (2010) and implemented in the software DoFEα. The method gives 95% confidence intervals for α_{EWK} and ωA_{EWK}, and the standard error associated with

the proportion of mutations in the four ranges of the DFE. Binning was necessary here, because estimations for single genes are imprecise. So we grouped genes into bins according to their value at each covariate (see "Covariates" section below), and DoFE was run for each bin independently. For numerical covariates, bins were based on quantiles that divide the data in equally sized groups.

The Direction of Selection, DoS

We calculated the direction of selection statistic (Stoletzki and Eyre-Walker 2011) as follows: $DoS = Dn/(Dn + Ds) - Pn/(Pn+Ps)$. A deficit of nonsynonymous polymorphisms relative to nonsynonymous substitutions ($DoS > 0$) indicates positive selection, whereas an excess of nonsynonymous polymorphisms relative to nonsynonymous substitutions ($DoS < 0$) is indicative of purifying selection. The correlation between ωA_{MK} and *DoS* was strong and highly significant ($\rho = 0.964$, *P*-value $<$ 2.2E-16, $n = 10{,}631$, supplementary fig. S1*a*, Supplementary Material online), as was to a lesser extent the correlation between α_{MK} and *DoS* ($\rho = 0.798$, *P*-value $<$ 2.2E-16, $n = 10{,}631$, supplementary fig. S1*a*, Supplementary Material online) and α_{MK} and ωA_{MK} ($\rho = 0.676$, *P*-value $<$ 2.2E-16, $n = 10{,}631$, supplementary fig. S1*a*, Supplementary Material online).

Covariates

We used the following statistics for each gene as covariates: 1) chromosomal location (autosome vs. X chromosome), 2) length of its longest transcript, 3) recombination rate, 4) global expression level (average expression of a gene over the whole body samples), 5) intersexual genetic correlation in expression, 6) sexual antagonism, 7) four types of connectivities, and 8) six types of expression specificities across sexes, life stages, and tissues. In the Supplementary Material online, we additionally considered the global selection strength (*Dn*/*Ds* in coding regions, and *Du*/*Ds* in noncoding regions). The final data sets including all covariates, α_{MK}, ωA_{MK}, and *DoS* estimates for each gene are provided in supplementary file S7, Supplementary Material online (coding sites excluding variants below 5%) and supplementary file S8, Supplementary Material online (noncoding sites excluding variants below 5%). Similarly, we provide in supplementary file S9, Supplementary Material online, the estimates for α_{EWK}, ωA_{EWK}, and the deleterious DFE obtained with the Eyre-Walker and Keightley method on binned data. In the following sections, details on the covariates are given.

Recombination Rate

We used a fine-scale recombination map of *D. melanogaster* statistically inferred based on population data from Gikongoro in Rwanda (Africa) and provided by Chan et al. (2012). The recombination rate for a gene was calculated as the mean rate (in units of *4*Ne*r* per bp) across all bins (defined as a window between each pair of successive single nucleotide polymorphisms) that a gene contains.

Intersexual Genetic Correlation in Expression

We used expression data in males and females quantified by genome-tiling microarrays in inbred lines of *D. melanogaster* from Raleigh in North Carolina and provided by Huang et al. (2015; http://dgrp2.gnets.ncsu.edu/data.html; last accessed October 2017). The intersexual genetic correlation in expression was then estimated for each gene using a bivariate mixed effects model with the TYPE = UNR option in Proc MIXED from SAS v.9.4 (following Allen et al. 2018; https://doi.org/10.6084/m9.figshare.c.4181168.v1; last accessed October 2018).

Sexual Antagonism

A list of candidate sexually antagonistic genes in *D. melanogaster* (LH_m strain) was obtained from Innocenti and Morrow (2010, table S1 sheet 4, doi: 10.1371/journal.pbio.1000335.s004). These genes are characterized by a significant *sex-by-fitness* interaction in a linear mixed model that partitions the variance in gene expression in different components: *sex effect*, *line fitness effect*, *batch effect*, and *sex-by-fitness interaction*. As previously found (Griffin et al. 2013), sexually antagonistic genes were characterized by a higher intersexual genetic correlation (median: $IC_{SAG} = 0.783$) than other genes (median: $IC_{non\text{-}SAG} = 0.610$) and this difference was significant (Wilcoxon's rank test: *P*-value = 1.77E-07, $n_{non\text{-}SAG} = 9{,}622$, $n_{SAG} = 1{,}009$).

We performed a supplementary analysis (supplementary fig. S7, Supplementary Material online) by considering only sexually antagonistic genes that additionally have a significant and opposite *fitness* effect in the sex-specific data sets (table S1 sheet 1 and 2 of Innocenti and Morrow 2010). However, we could not detect any significant effect of these genes, which may be due to the reduced sample sizes ($n = 68$ in coding regions, and $n = 66$ in noncoding regions).

Gene Connectivity

Gene connectivity was assessed based on the *Drosophila* Interactions Database (Murali et al. 2011) available from http://www.droidb.org (last accessed in October 2017). We calculated for each gene the number of interactions in which it was involved at four different levels: 1) genetic interactions ("fly_genetic_interactions.txt") which represent interactions between two alleles, 2) protein–protein interactions ("flybase_ppi.txt") which include experimentally derived physical interactions, 3) microRNA–gene interactions ("rna_gene.txt") which include predicted regulatory interactions, and 4) TF–gene interactions ("tf_gene.txt") which contain experimentally validated interactions.

Sex Specificity

For sex specificity, we estimated the sex-bias ratio as SBR = log2(RPKM♀/RPKM♂) based on whole body samples of female adults ("AdF_Ecl_1days," "AdF_Ecl_5days," "AdF_Ecl_30days") and male adults ("AdM_Ecl_1days," "AdM_Ecl_5days," "AdM_Ecl_30days"), and we calculated a folded sex specificity metric by taking the absolute value of the sex-bias ratio. Alternatively (supplementary fig. S4, Supplementary Material online), sex specificity was calculated

based on reproductive tissue samples in females ("A_VirF_4d_ovary," "A_MateF_4d_ovary") and males ("A_MateM_4d_acc_gland," "A_MateM_4d_testis"). Genes were also categorized in nine sex-bias bins depending on the value of the ratio: 1) male-specific if SBR < -8; 2) three male-biased classes if $-8 \leq$ SBR < -4, $-4 \leq$ SBR < -2, $-2 \leq$ SBR < -1; 3) three female-biased classes if $8 \geq$ SBR > 4, $4 \geq$ SBR > 2, $2 \geq$ SBR > 1; 4) female-specific if SBR > 8; and 5) unbiased if $-1 \leq$ SBR ≤ 1. Expression values of the different samples within each sex were averaged.

Developmental Stage/Tissue Specificities

We quantify the breadth of expression of a gene across different developmental stages and/or tissues by computing the expression bias (Yanai et al. 2005):

$$\tau = \frac{\sum_{j=1}^{n} 1 - \log(S_i)/\log(S_{max})}{n-1} \quad (1)$$

Here, n is the total number of stages/tissues, Sj is the expression level in stage/tissue j and $Smax$ is the largest expression level over all stages/tissues. We used τ to classify genes in different bins based on quantiles that divide the data into equally sized groups from broadly expressed ($\tau = 0$) to highly specific ($\tau = 1$) genes. Stage specificity was calculated based on whole body samples of four developmental stages: 1) embryos ("em2.4hr," "em4.6hr," "em6.8hr," "em8.10hr," "em10.12hr," "em12.14hr," "em14.16hr," "em16.18hr," "em18.20hr," "em20.22hr," and "em22.24hr"); 2) larvae ("L1," "L2," "L3_12hr," "L3_PS1.2," "L3_PS3.6," and "L3_PS7.9"); 3) pupae ("P5," "P6," "P8," "P9.10," and "P15"); and 4) adults ("AdF_Ecl_1days," "AdF_Ecl_5days," "AdF_Ecl_30days," "AdM_Ecl_1days," and "AdM_Ecl_5days"). Tissue specificity within larvae was calculated based on four tissues: 1) carcass ("L3_Wand_carcass"); 2) digestive system ("L3_Wand_dig_sys"); 3) CNS ("L3_CNS"); and 4) imaginal discs ("L3_Wand_imag_disc"). Tissue specificity within pupae was calculated based on two tissues: 1) CNS ("P8_CNS") and 2) fat ("P8_fat"). Somatic tissue-specificity within adults was calculated based on three tissues: 1) carcass ("A_1d_carcass," "A_4d_carcass," and "A_20d_carcass"); 2) digestive system ("A_1d_dig_sys," "A_4d_dig_sys," and "A_20d_dig_sys"); and 3) heads ("A_VirF_1d_head," "A_VirF_4d_head," "A_VirF_20d_head," "A_MateF_1d_head," "A_MateF_4d_head," "A_MateF_20d_head," "A_MateM_1d_head," "A_MateM_4d_head," and "A_MateM_20d_head"). Finally, we computed a "tissue-by-stage" specificity measure based on the four larval tissues, the two pupae tissues, and the three adult tissues. Expression values of the different samples within each stage/tissue were averaged.

Statistical Analyses

All statistical analyses were performed using the R version 3.3.1 (R Core Team 2016).

Single Covariate-Related Statistics

Confidence intervals were obtained by bootstrapping across genes (1,000 replicates) using the R function "boot" (from the package "boot"), and we report the 95% confidence intervals as ± 2 SD of the distribution of bootstrapped values. Differences in α_{MK} values for the categorical covariates (chromosomal location, sexual antagonism, and the nine sex specificity bins) were assessed with Wilcoxon's rank-sum tests (R function "wilcox.test" in package "stats"). For numerical covariates, we grouped genes into bins based on quantiles that divide the data into equally sized groups. We then calculated the Spearman's rank correlation between the median of the covariate at each bin and the median α_{MK} using the R function "cor.test" (from the package "stats"). We also fit least-squares linear regressions in the form $\alpha_{MK} \sim covariate$, and least-squares quadratic regressions in the form $\alpha_{MK} \sim covariate + covariate^2$ on unbinned data, calling the R function "lm" (from the R package "stats"). Model fits were then compared based on AIC (supplementary tables S1 and S2, Supplementary Material online).

Multicollinearity among Covariates

We performed a quantitative assessment of the relationships between covariates on unbinned data. First, Spearman's pairwise correlations were computed with the R function "cor.test" (from the package "stats") between α_{MK}, *DoS*, ωA_{MK}, and all numerical covariates (supplementary fig. S1*a*, Supplementary Material online). Second, a principal component analysis on all covariates was carried out with the R function "PCA" (from the package "FactoMineR," supplementary fig. S1*b*, Supplementary Material online). Numerical covariates were scaled to zero mean and unit variance. In both analyses, the five stage/tissue expression specificities proved to be nonindependent, and so we removed them all from subsequent investigations, except for the combined metric tissue-by-stage specificity. Computation of the variance inflation factors (R function "ols_vif_tol" in package "olsrr") in the linear models on *DoS* confirmed that the remaining 12 covariates had limited collinearity (supplementary tables S3 and S4, Supplementary Material online).

Multiple Linear Regression

We constructed linear models on unbinned data with the R function "lm" (from the package "stats") to analyze the relative contribution of the different covariates on the efficacy of selection. We analyzed separately *DoS* and ωA_{MK} as the response variables (they were chosen instead of α because *DoS* and ωA_{MK} follow the assumptions required by linear regressions, which α does not), and we compared two alternative sets of covariates. First, only the general modulators were included, as follows: *DoS* (respectively ωA_{MK}) $\sim$ *chromosomal location* + log(*transcript length*) + log(*recombination rate*) + log(*global expression level*). Then, we included the eight noncollinear pleiotropic covariates described in the previous section: *gene–gene interactions* + *protein–protein interactions* + *microRNA–gene interactions* + *TF–gene interactions* + *sexual antagonistic genes* + *intersexual genetic*

correlation + folded sex specificity + tissue-by-stage specificity. In both cases, residuals were independent, identically distributed and followed a Gaussian distribution of null mean (*DoS*: supplementary fig. S9*a*, Supplementary Material online; ωA_{MK}: supplementary fig. S9*b*, Supplementary Material online). Estimate of the effect of each covariate, its standard error, and significance were computed using the type III ANOVA implemented in the R function "Anova" (from the package "car"). The two linear models ("*general modulators only*" vs. "*all covariates*") were compared based on a likelihood ratio test using the R function "lrtest" (from package "lmtest"). Additionally, we carried out a stepwise model selection to eliminate step by step the covariates that contribute the least to the model, based on AIC comparison (table 2). We used the R function "stepAIC" (from the MASS package) including both direction of selection (forward and backward).

Partial Correlations and Principal Component Regression

As α was not suitable for a linear regression analysis, and many covariates were correlated with one another (supplementary fig. S1, Supplementary Material online), which can lead to imprecise estimates of individual effects in linear models, we alternatively calculated Spearman's rank partial correlations on unbinned data between α (respectively *DoS* and ωA_{MK}) and each covariate, conditional on all other covariates, using the R function "pcor.test" (from the package "ppcor," supplementary tables S3 and S4, Supplementary Material online).

To further overcome the issue of multicollinearity within a linear modeling framework, we performed a principal component regression on *DoS* (supplementary tables S5 and S6, Supplementary Material online). We first identified the independent source of variation in the data using a principal component analysis on all 12 covariates. Then, we performed a linear regression of *DoS* on the principal components to obtain an estimate of the effect of each principal component and its significance. Covariates basically show the same ordering regarding their contribution to the variance in *DoS* as in the linear models on the original covariates.

Supplementary Material

Supplementary data are available at *Molecular Biology and Evolution* online.

Acknowledgments

We are grateful to Brian Charlesworth, Nicolas Bierne, and two anonymous reviewers for insightful comments on the article. The computations were performed with the IST Austria HPC cluster, and we are particularly grateful to Janos Kiss and Alois Schloegl for their help. This work was funded by an Austrian Science Foundation FWF grant (Project P 28842) to B.V., and C.F. was supported by an IST fellow (IST Austria and Marie Sklodowska-Curie Co-Funding European program).

References

Allen SL, Bonduriansky R, Chenoweth SF. 2018. Genetic constraints on microevolutionary divergence of sex-biased gene expression. *Philos Trans R Soc Lond B Biol Sci*. 373(1757): 20170427.

Allen SL, Bonduriansky R, Sgro CM, Chenoweth SF. 2017. Sex-biased transcriptome divergence along a latitudinal gradient. *Mol Ecol*. 26(5): 1256–1272.

Andolfatto P. 2005. Adaptive evolution of non-coding DNA in *Drosophila*. *Nature* 437(7062): 1149–1152.

Andolfatto P, Wong KM, Bachtrog D. 2011. Effective population size and the efficacy of selection on the X chromosomes of two closely related *Drosophila* species. *Genome Biol Evol*. 3:114–128.

Arnqvist G, Tuda M. 2010. Sexual conflict and the gender load: correlated evolution between population fitness and sexual dimorphism in seed beetles. *Proc R Soc Lond B Biol Sci*. 277(1686): 1345–1352.

Artieri CG, Haerty W, Singh RS. 2009. Ontogeny and phylogeny: molecular signatures of selection, constraint, and temporal pleiotropy in the development of *Drosophila*. *BMC Biol*. 7:42.

Assis R, Zhou Q, Bachtrog D. 2012. Sex-biased transcriptome evolution in *Drosophila*. *Genome Biol Evol*. 4(11): 1189–1200.

Avila V, Campos JL, Charlesworth B. 2015. The effects of sex-biased gene expression and X-linkage on rates of adaptive protein sequence evolution in *Drosophila*. *Biol Lett*. 11(4): 20150117.

Bachtrog D. 2008. Similar rates of protein adaptation in *Drosophila miranda* and *D. melanogaster*, two species with different current effective population sizes. *BMC Evol Biol*. 8(1): 334.

Barrett LW, Fletcher S, Wilton SD. 2012. Regulation of eukaryotic gene expression by the untranslated gene regions and other non-coding elements. *Cell Mol Life Sci*. 69(21): 3613–3634.

Bataillon T, Duan J, Hvilsom C, Jin X, Li Y, Skov L, Glemin S, Munch K, Jiang T, Qian Y, et al. 2015. Inference of purifying and positive selection in three subspecies of chimpanzees (*Pan troglodytes*) from exome sequencing. *Genome Biol Evol*. 7(4): 1122–1132.

Betancourt AJ, Presgraves DC. 2002. Linkage limits the power of natural selection in *Drosophila*. *Proc Natl Acad Sci U S A*. 99(21): 13616–13620.

Bierne N, Eyre-Walker A. 2004. The genomic rate of adaptive amino acid substitution in *Drosophila*. *Mol Biol Evol*. 21(7): 1350–1360.

Bolívar P, Mugal CF, Nater A, Ellegren H. 2016. Recombination rate variation modulates gene sequence evolution mainly via GC-biased gene conversion, not Hill–Robertson interference, in an avian system. *Mol Biol Evol*. 33(1): 216–227.

Bolstad B. 2017. preprocessCore: a collection of pre-processing functions. R package version 1.40.0. Available from: https://github.com/bmbolstad/preprocessCore.

Bonduriansky R, Chenoweth SF. 2009. Intralocus sexual conflict. *Trends Ecol Evol*. 24(5): 280–288.

Booker TR, Jackson BC, Keightley PD. 2017. Detecting positive selection in the genome. *BMC Biol*. 15(1): 98.

Booker TR, Keightley PD. 2018. Understanding the factors that shape patterns of nucleotide diversity in the house mouse genome. *Mol Biol Evol*. 35(12):2971–2988.

Campos JL, Halligan DL, Haddrill PR, Charlesworth B. 2014. The relation between recombination rate and patterns of molecular evolution and variation in *Drosophila melanogaster*. *Mol Biol Evol*. 31(4): 1010–1028.

Campos JL, Johnston K, Charlesworth B. 2018. The effects of sex-biased gene expression and X-linkage on rates of sequence evolution in *Drosophila*. *Mol Biol Evol*. 35(3): 655–665.

Campos JL, Zhao L, Charlesworth B. 2017. Estimating the parameters of background selection and selective sweeps in *Drosophila* in the presence of gene conversion. *Proc Natl Acad Sci U S A*. 114(24): E4762–E4771.

Carneiro M, Albert FW, Melo-Ferreira J, Galtier N, Gayral P, Blanco-Aguiar JA, Villafuerte R, Nachman MW, Ferrand N. 2012. Evidence for widespread positive and purifying selection across the European rabbit (*Oryctolagus cuniculus*) genome. *Mol Biol Evol*. 29(7): 1837–1849.

Castellano D, Coronado-Zamora M, Campos JL, Barbadilla A, Eyre-Walker A. 2016. Adaptive evolution is substantially impeded by Hill-Robertson interference in *Drosophila*. *Mol Biol Evol*. 33(2): 442–455.
Chan AH, Jenkins PA, Song YS. 2012. Genome-wide fine-scale recombination rate variation in *Drosophila melanogaster*. *PLoS Genet*. 8(12): e1003090.
Charlesworth B, Campos JL. 2014. The relations between recombination rate and patterns of molecular variation and evolution in *Drosophila*. *Annu Rev Genet*. 48:383–403.
Charlesworth B, Campos JL, Jackson BC. 2018. Faster-X evolution: theory and evidence from *Drosophila*. *Mol Ecol*. 27(19): 3753–3771.
Charlesworth B, Coyne JA, Barton NH. 1987. The relative rates of evolution of sex chromosomes and autosomes. *Am Nat*. 130(1): 113–146.
Charlesworth J, Eyre-Walker A. 2008. The McDonald-Kreitman test and slightly deleterious mutations. *Mol Biol Evol*. 25(6): 1007–1015.
Cingolani P, Platts A, Wang LL, Coon M, Nguyen T, Wang L, Land SJ, Lu X, Ruden DM. 2012. A program for annotating and predicting the effects of single nucleotide polymorphisms, SnpEff: SNPs in the genome of *Drosophila melanogaster* strain w1118; Iso-2; Iso-3. *Fly* 6(2): 80–92.
Collet JM, McGuigan K, Allen SL, Chenoweth SF, Blows MW. 2018. Mutational pleiotropy and the strength of stabilizing selection within and between functional modules of gene expression. *Genetics* 208(4): 1601–1616.
Connallon T, Clark AG. 2011. Association between sex-biased gene expression and mutations with sex-specific phenotypic consequences in *Drosophila*. *Genome Biol Evol*. 3:151–155.
Connallon T, Hall MD. 2018. Genetic constraints on adaptation: a theoretical primer for the genomics era. *Ann N Y Acad Sci*. 1422(1): 65–87.
Cutter AD, Ward S. 2005. Sexual and temporal dynamics of molecular evolution in *C. elegans* development. *Mol Biol Evol*. 22(1): 178–188.
Danecek P, Auton A, Abecasis G, Albers CA, Banks E, DePristo MA, Handsaker RE, Lunter G, Marth GT, Sherry ST, et al. 2011. The variant call format and VCFtools. *Bioinformatics* 27(15): 2156–2158.
Darwin C. 1871. The descent of man, and selection in relation to sex. London: John Murray.
Davis JC, Brandman O, Petrov DA. 2005. Protein evolution in the context of *Drosophila* development. *J Mol Evol*. 60(6): 774–785.
Dean R, Mank JE. 2016. Tissue specificity and sex-specific regulatory variation permit the evolution of sex-biased gene expression. *Am Nat*. 188(3): E74–E84.
Duret L, Mouchiroud D. 2000. Determinants of substitution rates in mammalian genes: expression pattern affects selection intensity but not mutation rate. *Mol Biol Evol*. 17(1): 68–74.
Ellegren H, Parsch J. 2007. The evolution of sex-biased genes and sex-biased gene expression. *Nat Rev Genet*. 8(9): 689–698.
Elyashiv E, Sattath S, Hu TT, Strutsovsky A, McVicker G, Andolfatto P, Coop G, Sella G. 2016. A genomic map of the effects of linked selection in *Drosophila*. *PLoS Genet*. 12(8): e1006130.
Eyre-Walker A, Keightley PD. 2009. Estimating the rate of adaptive molecular evolution in the presence of slightly deleterious mutations and population size change. *Mol Biol Evol*. 26(9): 2097–2108.
Eyre-Walker A, Woolfit M, Phelps T. 2006. The distribution of fitness effects of new deleterious amino acid mutations in humans. *Genetics* 173(2): 891–900.
Fay JC, Wyckoff GJ, Wu CI. 2001. Positive and negative selection on the human genome. *Genetics* 158(3): 1227–1234.
Fisher RA. 1930. The genetical theory of natural selection. Oxford: Oxford University Press.
Galtier N. 2016. Adaptive protein evolution in animals and the effective population size hypothesis. *PLoS Genet*. 12(1): e1005774.
Good JM, Nachman MW. 2005. Rates of protein evolution are positively correlated with developmental timing of expression during mouse spermatogenesis. *Mol Biol Evol*. 22(4): 1044–1052.
Gossmann TI, Song BH, Windsor AJ, Mitchell-Olds T, Dixon CJ, Kapralov MV, Filatov DA, Eyre-Walker A. 2010. Genome wide analyses reveal little evidence for adaptive evolution in many plant species. *Mol Biol Evol*. 27(8): 1822–1832.
Grath S, Parsch J. 2012. Rate of amino acid substitution is influenced by the degree and conservation of male-biased transcription over 50 Myr of *Drosophila* evolution. *Genome Biol Evol*. 4(3): 346–359.
Griffin RM, Dean R, Grace JL, Rydén P, Friberg U. 2013. The shared genome is a pervasive constraint on the evolution of sex-biased gene expression. *Mol Biol Evol*. 30(9): 2168–2176.
Haddrill PR, Halligan DL, Tomaras D, Charlesworth B. 2007. Reduced efficacy of selection in regions of the *Drosophila* genome that lack crossing over. *Genome Biol*. 8(2): R18.
Hahn MW, Conant GC, Wagner A. 2004. Molecular evolution in large genetic networks: does connectivity equal constraint? *J Mol Evol*. 58(2): 203–211.
Hahn MW, Kern AD. 2005. Comparative genomics of centrality and essentiality in three eukaryotic protein-interaction networks. *Mol Biol Evol*. 22(4): 803–806.
Haldane JBS. 1927. A mathematical theory of natural and artificial selection, Part V: selection and mutation. *Math Proc Camb Philos Soc*. 23(07): 838.
He X, Zhang J. 2006. Toward a molecular understanding of pleiotropy. *Genetics* 173(4): 1885–1891.
Hill WG, Robertson A. 1966. The effect of linkage on limits to artificial selection. *Genet Res*. 8(03): 269.
Hill WG, Zhang XS. 2012. On the pleiotropic structure of the genotype–phenotype map and the evolvability of complex organisms. *Genetics* 190(3):1131–1137.
Huang W, Carbone MA, Magwire MM, Peiffer JA, Lyman RF, Stone EA, Anholt RRH, Mackay TFC. 2015. Genetic basis of transcriptome diversity in *Drosophila melanogaster*. *Proc Natl Acad Sci U S A*. 112(44): E6010–E6019.
Huber CD, Kim BY, Marsden CD, Lohmueller KE. 2017. Determining the factors driving selective effects of new nonsynonymous mutations. *Proc Natl Acad Sci U S A*. 114(17): 4465–4470.
Huylmans AK, Parsch J. 2014. Population-and sex-biased gene expression in the excretion organs of *Drosophila melanogaster*. *G3 (Bethesda)* 4(12): 2307–2315.
Innocenti P, Morrow EH. 2010. The sexually antagonistic genes of *Drosophila melanogaster*. *PLoS Biol*. 8(3): e1000335.
Jensen JD, Bachtrog D. 2011. Characterizing the influence of effective population size on the rate of adaptation: Gillespie's Darwin domain. *Genome Biol Evol*. 3(0): 687–701.
Jordan IK, Wolf YI, Koonin EV. 2003. No simple dependence between protein evolution rate and the number of protein-protein interactions: only the most prolific interactors tend to evolve slowly. *BMC Evol Biol*. 3:1.
Josephs EB, Wright SI, Stinchcombe JR, Schoen DJ. 2017. The relationship between selection, network connectivity, and regulatory variation within a population of *Capsella grandiflora*. *Genome Biol Evol*. 9(4): 1099–1109.
Kayserili MA, Gerrard DT, Tomancak P, Kalinka AT. 2012. An excess of gene expression divergence on the X chromosome in *Drosophila* embryos: implications for the Faster-X hypothesis. *PLoS Genet*. 8(12): e1003200.
Kimura M, Ohta T. 1971. Theoretical aspects of population genetics. Princeton (NJ): Princeton University Press.
Kimura M, Ohta T. 1974. On some principles governing molecular evolution. *Proc Natl Acad Sci U S A*. 71(7): 2848–2852.
Lack JB, Cardeno CM, Crepeau MW, Taylor W, Corbett-Detig RB, Stevens KA, Langley CH, Pool JE. 2015. The *Drosophila* genome nexus: a population genomic resource of 623 *Drosophila melanogaster* genomes, including 197 from a single ancestral range population. *Genetics* 199(4): 1229–1241.
Larracuente AM, Sackton TB, Greenberg AJ, Wong A, Singh ND, Sturgill D, Zhang Y, Oliver B, Clark AG. 2008. Evolution of protein-coding genes in *Drosophila*. *Trends Genet*. 24(3): 114–123.
Lawrie DS, Messer PW, Hershberg R, Petrov DA. 2013. Strong purifying selection at synonymous sites in *D. melanogaster*. *PLoS Genet*. 9(5): e1003527.

Lemaître JF, Berger V, Bonenfant C, Douhard M, Gamelon M, Plard F, Gaillard JM. 2015. Early-late life trade-offs and the evolution of ageing in the wild. *Proc R Soc B*. 282(1806): 20150209.
Lipinska A, Cormier A, Luthringer R, Peters AF, Corre E, Gachon CMM, Cock JM, Coelho SM. 2015. Sexual dimorphism and the evolution of sex-biased gene expression in the brown alga *Ectocarpus*. *Mol Biol Evol*. 32(6): 1581–1597.
Mank JE, Hultin-Rosenberg L, Zwahlen M, Ellegren H. 2008. Pleiotropic constraint hampers the resolution of sexual antagonism in vertebrate gene expression. *Am Nat*. 171(1): 35–43.
Marad DA, Buskirk SW, Lang GI. 2018. Altered access to beneficial mutations slows adaptation and biases fixed mutations in diploids. *Nat Ecol Evol*. 2(5): 882.
Matsumoto T, John A, Baeza-Centurion P, Li B, Akashi H. 2016. Codon usage selection can bias estimation of the fraction of adaptive amino acid fixations. *Mol Biol Evol*. 33(6): 1580–1589.
Maynard SJ. 1976. What determines the rate of evolution? *Am Nat*. 110(973): 331–338.
McDonald JH, Kreitman M. 1991. Adaptive protein evolution at the Adh locus in *Drosophila*. *Nature* 351(6328): 652–654.
McGuigan K, Collet JM, Allen SL, Chenoweth SF, Blows MW. 2014. Pleiotropic mutations are subject to strong stabilizing selection. *Genetics* 197(3): 1051–1062.
McVean GA, Vieira J. 2001. Inferring parameters of mutation, selection and demography from patterns of synonymous site evolution in *Drosophila*. *Genetics* 157(1): 245–257.
Meisel RP. 2011. Towards a more nuanced understanding of the relationship between sex-biased gene expression and rates of protein-coding sequence evolution. *Mol Biol Evol*. 28(6): 1893–1900.
Meisel RP, Connallon T. 2013. The Faster-X effect: integrating theory and data. *Trends Genet*. 29(9): 537–544.
Meisel RP, Malone JH, Clark AG. 2012. Faster-X evolution of gene expression in *Drosophila*. *PLoS Genet*. 8(10): e1003013.
Messer PW, Petrov DA. 2013. Frequent adaptation and the McDonald-Kreitman test. *Proc Natl Acad Sci U S A*. 110(21): 8615–8620.
modENCODE Consortium. 2010. Identification of functional elements and regulatory circuits by *Drosophila* modENCODE. *Science* 330(6012): 1787–1797.
Müller L, Grath S, von Heckel K, Parsch J. 2012. Inter-and intraspecific variation in *Drosophila* genes with sex-biased expression. *Int J Evol Biol*. 2012:963976.
Murali T, Pacifico S, Yu J, Guest S, Roberts GG, Finley RL. 2011. DroID 2011: a comprehensive, integrated resource for protein, transcription factor, RNA and gene interactions for *Drosophila*. *Nucleic Acids Res*. 39(Database issue): D736–D743.
Muyle A, Martin H, Zemp N, Mollion M, Gallina S, Tavares R, Silva A, Bataillon T, Widmer A, Glemin S, et al. 2018. Dioecy in plants: an evolutionary dead end? Insights from a population genomics study in the *Silene* genus. *bioRxiv* 414771.
Nei M, Maruyama T, Chakraborty R. 1975. The bottleneck effect and genetic variability in populations. *Evolution* 29(1): 1.
Nelson CW, Moncla LH, Hughes AL. 2015. SNPGenie: estimating evolutionary parameters to detect natural selection using pooled next-generation sequencing data. *Bioinformatics* 31(22): 3709–3711.
Nourmohammad A, Rambeau J, Held T, Kovacova V, Berg J, Lässig M. 2017. Adaptive evolution of gene expression in *Drosophila*. *Cell Rep*. 20(6): 1385–1395.
Obbard DJ, Welch JJ, Kim KW, Jiggins FM. 2009. Quantifying adaptive evolution in the *Drosophila* immune system. *PLoS Genet*. 5(10): e1000698.
Ohya Y, Sese J, Yukawa M, Sano F, Nakatani Y, Saito TL, Saka A, Fukuda T, Ishihara S, Oka S, et al. 2005. High-dimensional and large-scale phenotyping of yeast mutants. *Proc Natl Acad Sci U S A*. 102(52): 19015–19020.
Paaby AB, Rockman MV. 2013. The many faces of pleiotropy. *Trends Genet*. 29(2): 66–73.
Page AJ, Keane JA, Delaney AJ, Taylor B, Seemann T, Harris SR, Soares J. 2016. SNP-sites: rapid efficient extraction of SNPs from multi-FASTA alignments. *Microb Genom*. 2(4): e000056.
Pál C, Papp B, Lercher MJ. 2006. An integrated view of protein evolution. *Nat Rev Genet*. 7(5): 337–348.
Papakostas S, Vøllestad LA, Bruneaux M, Aykanat T, Vanoverbeke J, Ning M, Primmer CR, Leder EH. 2014. Gene pleiotropy constrains gene expression changes in fish adapted to different thermal conditions. *Nat Commun*. 5:4071.
Parsch J, Ellegren H. 2013. The evolutionary causes and consequences of sex-biased gene expression. *Nat Rev Genet*. 14(2): 83–87.
Perry JC, Harrison PW, Mank JE. 2014. The ontogeny and evolution of sex-biased gene expression in *Drosophila melanogaster*. *Mol Biol Evol*. 31(5): 1206–1219.
Pool JE, Corbett-Detig RB, Sugino RP, Stevens KA, Cardeno CM, Crepeau MW, Duchen P, Emerson JJ, Saelao P, Begun DJ, et al. 2012. Population genomics of sub-Saharan *Drosophila melanogaster*: African diversity and non-African admixture. *PLoS Genet*. 8(12): e1003080.
Presgraves DC. 2005. Recombination enhances protein adaptation in *Drosophila melanogaster*. *Curr Biol*. 15(18): 1651–1656.
Promislow DEL. 2004. Protein networks, pleiotropy and the evolution of senescence. *Proc R Soc Lond B Biol Sci*. 271(1545): 1225–1234.
Pröschel M, Zhang Z, Parsch J. 2006. Widespread adaptive evolution of *Drosophila* genes with sex-biased expression. *Genetics* 174(2): 893–900.
R Core Team. 2016. R: A language and environment for statistical computing. Vienna, Austria: R Foundation for Statistical Computing. https://www.R-project.org/.
Rice WR. 1992. Sexually antagonistic genes: experimental evidence. *Science* 256(5062): 1436–1439.
Rose M, Charlesworth B. 1980. A test of evolutionary theories of senescence. *Nature* 287(5778): 141–142.
Salathé M, Ackermann M, Bonhoeffer S. 2006. The effect of multifunctionality on the rate of evolution in yeast. *Mol Biol Evol*. 23(4): 721–722.
Smith NG, Eyre-Walker A. 2002. Adaptive protein evolution in *Drosophila*. *Nature* 415(6875): 1022.
Stoletzki N, Eyre-Walker A. 2011. Estimation of the neutrality index. *Mol Biol Evol*. 28(1): 63–70.
Torgerson DG, Kulathinal RJ, Singh RS. 2002. Mammalian sperm proteins are rapidly evolving: evidence of positive selection in functionally diverse genes. *Mol Biol Evol*. 19(11): 1973–1980.
Van Dyken JD, Wade MJ. 2010. The genetic signature of conditional expression. *Genetics* 184(2): 557–570.
VanKuren NW, Long M. 2018. Gene duplicates resolving sexual conflict rapidly evolved essential gametogenesis functions. *Nat Ecol Evol*. 2(4): 705.
Vedanayagam JP, Garrigan D. 2015. The effects of natural selection across molecular pathways in *Drosophila melanogaster*. *BMC Evol Biol*. 15(1): 203.
Vicoso B, Charlesworth B. 2009. Effective population size and the Faster-X effect: an extended model. *Evolution* 63(9): 2413–2426.
Wagner GP, Kenney-Hunt JP, Pavlicev M, Peck JR, Waxman D, Cheverud JM. 2008. Pleiotropic scaling of gene effects and the 'cost of complexity'. *Nature* 452(7186): 470–472.
Wagner GP, Zhang J. 2011. The pleiotropic structure of the genotype-phenotype map: the evolvability of complex organisms. *Nat Rev Genet*. 12(3): 204–213.
Williams GC. 1957. Pleiotropy, natural selection, and the evolution of senescence. *Evolution* 11(4): 398.
Yanai I, Benjamin H, Shmoish M, Chalifa-Caspi V, Shklar M, Ophir R, Bar-Even A, Horn-Saban S, Safran M, Domany E, et al. 2005. Genome-wide midrange transcription profiles reveal expression level relationships in human tissue specification. *Bioinformatics* 21(5): 650–659.
Zhang Z, Hambuch TM, Parsch J. 2004. Molecular evolution of sex-biased genes in *Drosophila*. *Mol Biol Evol*. 21(11): 2130–2139.
Zhang Z, Parsch J. 2005. Positive correlation between evolutionary rate and recombination rate in *Drosophila* genes with male-biased expression. *Mol Biol Evol*. 22(10): 1945–1947.